

RESEARCH ARTICLE

*Don't Deny Your Inner Environmental Physiologist: Investigating Physiology with Environmental Stimuli***Identification of therapeutic targets in a murine model of severe exertional heat stroke****Kentaro Oki,¹ Chloe G. Henderson,^{1,2} Shauna M. Ward,¹ Jermaine A. Ward,¹ Mark L. Plamper,¹ Thomas A. Mayer,¹ Aaron R. Caldwell,^{1,2} and Lisa R. Leon¹**¹Thermal and Mountain Medicine Division, United States Army Research Institute of Environmental Medicine, Natick, Massachusetts and ²Oak Ridge Institute of Science and Education, Oak Ridge, Tennessee**Abstract**

Exertional heat stroke (EHS) is a potentially lethal condition resulting from high core body temperatures (T_C) in combination with a systemic inflammatory response syndrome (SIRS) with varying degrees of severity across victims, and limited understanding of the underlying mechanism(s). We established a mouse model of severe EHS to identify mechanisms of hyperthermia/inflammation that may be responsible for organ damage. Mice were forced to run on a motorized wheel in a 37.5°C chamber until loss of consciousness and were either removed immediately (exertional heat injury or EHI; $T_{CMax} = 42.4 \pm 0.2^\circ\text{C}$) or remained in the chamber an additional 20 min (EHS; $T_{CMax} = 42.5 \pm 0.4^\circ\text{C}$). Exercise control mice (ExC) experienced identical procedures to EHS at 25°C. At 3 h post-EHS, there was evidence for an immune/inflammatory response as elevated blood chemokine [interferon γ -induced protein 10 (IP-10), keratinocytes-derived chemokine (KC), macrophage inflammatory proteins (MIP-1 α), MIP-1 β , MIP-2] and cytokine [granulocyte colony-stimulating factor (G-CSF), interleukins (IL-10), IL-6] levels peaked and were highest in EHS mice compared with EHI and ExC mice. Immunoblotting of organs susceptible to EHS damage indicated that several kinases were sensitive to stress associated with heat/inflammation and exercise; specifically, phosphorylation of liver c-Jun NH₂-terminal kinase (JNK) at threonine 183/tyrosine 185 immediately (0 h) postheating related to heat illness severity. We have established a mouse EHS model, and JNK [or its downstream target(s)] could underlie EHS symptomatology, allowing the identification of molecular pathways or countermeasure targets to mitigate heat illness severity, enable complete recovery, and decrease overall EHS-related fatalities.

*cytokine; exercise; heat stroke; kinase; stress***INTRODUCTION**

Exertional heat illnesses are categorized by gradations of increasing severity from heat exhaustion to exertional heat injury (EHI) and to exertional heat stroke (EHS) (1). However, a severe heat illness does not occur due to progression from a milder heat illness (i.e., heat exhaustion is not required to develop EHI or EHS; EHI is not required to develop EHS). EHS is the most serious heat illness, characterized by high core body temperature (T_C) and severe neurological alterations, including delirium, deep coma, and seizures (2–4) and can lead to death if not properly treated. In contrast to classic (or passive) heat stroke (CHS), EHS results from exercise/exertion in a temperate to hot environment with insufficient heat dissipation from the body. Consequently, whereas CHS is predominantly observed in sedentary individuals who cannot easily thermoregulate or

may be immunocompromised, such as extremely young and old patients, EHS typically affects young, active individuals who are otherwise healthy (1). In particular, military personnel, athletes, and occupational workers have high rates of EHS. There were 488 EHS cases among active component service members of the United States Armed Forces during 2021 (5), and the average in-patient cost for each EHS case from 2016 to 2018 was approximately \$7,453 (6). In the United States, EHS is one of the leading causes of sudden death during high school sports (7). Finally, between the years 2000 and 2010, there were 359 deaths of occupational workers in various sectors (e.g., agriculture, forestry, etc.), believed to be due to high levels of physical exertion in warm environments (8). Although deaths were not categorized by heat illness type, 71% of the 359 occurred on the day of heat exposure (8), suggesting some, if not a significant number, likely suffered and

succumbed to acute EHS effects rather than protracted adverse consequences following collapse.

The development of EHS is directly related to metabolic heat production from skeletal muscle contractions (9) and exertion in temperate to hot environmental temperatures which cause hyperthermia (10). During EHS, cytokines and chemokines are released into circulation, often leading to dysregulation of the inflammatory reaction and triggering an immune response throughout the body known as the systemic inflammatory response syndrome (SIRS). SIRS, in turn, can result in disseminated intravascular coagulation (DIC, abnormal blood clotting in the circulatory system), multiorgan failure, and ultimately death (11). Hepatic failure due to EHS can require liver transplants to allow full recovery (12–14) although this is not always successful (15, 16). Even after recovery, a single EHS may predispose an individual to later health issues. A study in Army basic trainees concluded that patients with EHS exhibited an approximately twofold increased risk of heart, kidney, or liver failure within ~30 yr of hospitalization and treatment relative to trainees who suffered appendicitis (17). A caveat is that this was an uncontrolled epidemiological study, and other lifestyle choices engaged by individuals following (and potentially before) EHS may have influenced outcomes (e.g., alcohol consumption led to liver failure in a higher proportion of EHS patients) (17, 18). However, the study underscores 1) the importance of the heart, kidneys, and liver during EHS pathophysiology, and 2) that it is vital to identify biomarkers or mechanisms of residual damage that may go undetected with current treatment practices, making patients with EHS more vulnerable to later chronic health issues and/or death.

To elucidate the events that lead to heat stroke onset and pathophysiology, animal models using passive and exertional heating have enabled quantitation and characterization of thermal profiles as well as cytokine/chemokine levels with both CHS and EHS (19–22). These models have characterized the thermoregulatory profiles, chemokine/cytokine responses, and characteristics of organ injury, but the exertional studies were likely more representative of EHI than EHS due to no mortality, relatively rapid recovery, and even enhanced heat resistance in subsequent heating sessions (23). Establishment and characterization of a more severe EHS model in rodents are needed to provide a platform for testing potentially efficacious treatments that can prevent severe organ damage and assist with recovery in humans. We established controlled parameters for testing mice, which reliably and reproducibly induced an EHS phenotype and were distinct from previous work (24, 25). Accordingly, the purpose of the current study was twofold: 1) to establish a murine model of severe EHS (i.e., some level of mortality) and 2) to characterize the cytokine/chemokine profile and signaling proteins that distinguish it from the less severe condition of EHI. We also sought to characterize signaling proteins and/or inflammatory factors involved in stress response in organs that suffer extensive damage during EHS and are at risk for failure in patients with EHS decades later (17): the liver, kidneys, and heart. Characterizing the nodes potentially involved in EHS could lead to more targeted interventions to mitigate EHS severity, treat EHS symptomatology, and reduce fatalities/chronic health issues.

METHODS

Ethical Approval

All procedures were approved by the Institutional Animal Care and Use Committee. In conducting this research, the investigators adhered to the Guide for the Care and Use of Laboratory Animals in an Association for Assessment and Accreditation of Laboratory Animal Care-accredited facility.

Animals

Animal care was provided as previously described (26). Male C57BL/6J mice (6–8 wk old, 24 ± 1.6 g, Jackson Laboratories, Bar Harbor, ME) were individually housed at $25 \pm 2^\circ\text{C}$ and ~30% relative humidity (RH), 12:12 h light-dark cycle with lights on at 0600. Food and water were provided ad libitum except during training sessions and the forced running protocol. Each cage was supplied with enrichment, as described previously (26). Body core temperature (T_{c} ; $\pm 0.1^\circ\text{C}$) and general activity (counts) were measured with intraperitoneally (IP) implanted radiotelemetry transmitters (1.1 g, model G2 Emitter; Starr Life Sciences Corp., Inc., Oakmont, PA) (27). Surgical analgesia was provided with a subcutaneous injection of slow-release buprenorphine (0.05 mg/kg) just before surgery.

Experimental Approach

One week after telemeter implantation, running wheels were placed in cages to allow ad libitum voluntary running. Two days before the designated testing session, mice underwent 60 min of incremental exercise training sessions in forced running wheels (model 80840; Lafayette Instrument, Lafayette, IN) in an environmental chamber (model 3950; Thermo Forma, Marietta, OH) maintained at $25 \pm 2^\circ\text{C}$, relative humidity of ~30%. The training exercise started at 3.0 m/min and increased by 0.5 m/min every 10 min up to 5.5 m/min. Upon completion, mice were returned to their home cages for at least one wash-out day before testing, and the home cage running wheel was locked to avoid additional voluntary running or training effects. On the day before testing, mice in their home cages were placed into a floor-standing environmental chamber (model Forma 3940; Thermo Fisher, Marietta, OH) at $25 \pm 2^\circ\text{C}$ and ~30% RH; running wheels remained locked. The forced running protocol was similar to what has been described previously (26), except that the initial speed was 3.0 m/min and incrementally increased by 0.5 m/min every 10 min until the wheel speed reached 8.5 m/min right after 110 min; wheel speed was maintained at 8.5 m/min until mice lost consciousness.

A schematic for experimental groups is provided in Fig. 1. Mice that ran at 37.5°C were designated as EHI ($n = 54$) or EHS ($n = 63$). Each EHS specimen had a matched exercise control (ExC; $n = 63$). Upon collapse, EHS mice were removed from the wheel and left in another compartment of the chamber at 37.5°C for 20 min (passive phase). ExC animals underwent the same forced running protocol and 20 min of passive rest in the chamber at $T_{\text{Env}} = 25 \pm 2^\circ\text{C}$. All sample collection for ExC groups was time-matched to the EHS groups. Following the 20-min passive phase, EHS and ExC mice were weighed and euthanized immediately (0 h) or allowed to recover undisturbed at $T_{\text{Env}} = 25 \pm 2^\circ\text{C}$ with food and water

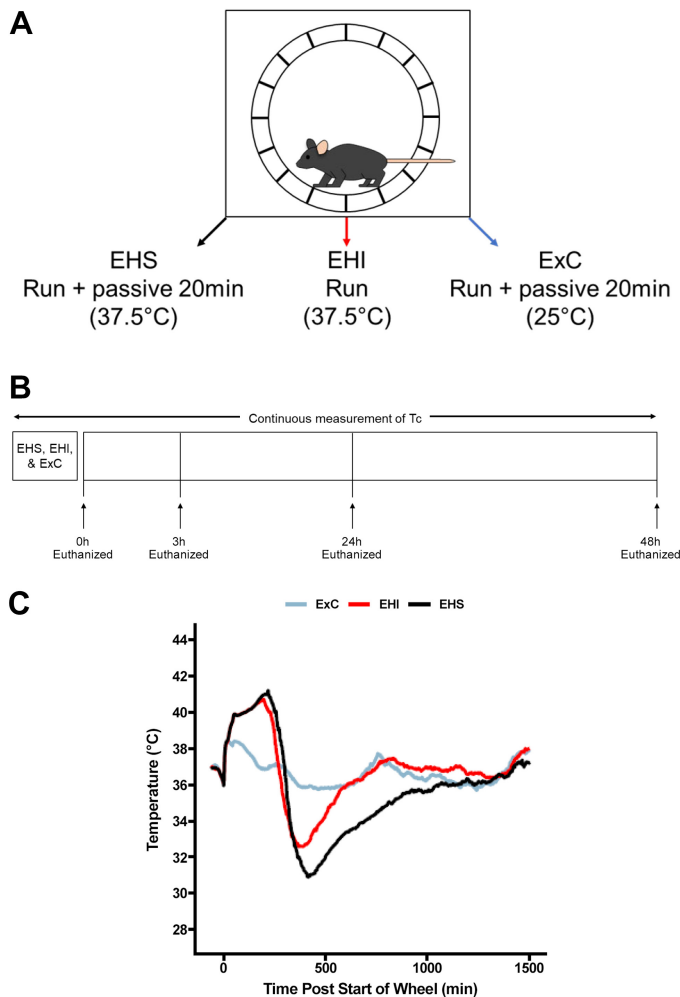


Figure 1. A: illustration of parameters for the three conditions. EHS mice ran on a motorized wheel in a chamber set at 37.5°C until collapse and remained in the same chamber for an additional 20 min to induce a more severe heat illness. An ExC was paired to each EHS mouse; each ExC mouse ran for an identical duration as its EHS counterpart in a chamber set at 25°C and upon run cessation, remained in its chamber for an additional 20 min. Similar to the EHS condition, EHI mice ran at 37.5°C until loss of consciousness but were immediately removed from the chamber upon collapse. B: timeline for animal conditions/euthanasia. Animals were euthanized at immediately after their protocol (0 h) and roughly around time of T_{CMin} for EHI/EHS (3 h), 24 h, and 48 h. Recovery for 3 h, 24 h, and 48 h occurred at a $T_{Env} = 25^\circ\text{C}$. C: thermal curves in ExC, EHI, and EHS mice. EHS mice attained higher maximal core temperature (T_{CMax}) and lower minimal core temperature (T_{CMin} – indicative of heat illness severity) compared with EHI mice. Chemokine/cytokine levels inversely corresponded to the T_c during hypothermia in mice following heating. The hypothermic phase around T_{CMin} corresponded to the period when chemokine/cytokine levels were elevated to peak levels in EHS and EHI mice with lower T_{CMin} and higher chemokines/cytokines in EHS mice. Although ExC mice also exhibited T_c fluctuations, their range of T_c was narrower than the ranges observed for EHS and EHI mice. ExC, exercise control; EHI, exertional heat injury; EHS, exertional heat stroke.

provided ad libitum in their home cages until sample collection at 3 h, 24 h, and 48 h post-protocol. EHI conditions were similar to previous studies (20, 21). Once collapsed, mice were weighed and immediately euthanized (0 h) or allowed to recover undisturbed at $T_{Env} = 25 \pm 2^\circ\text{C}$ with food and water provided ad libitum in their home cages until sample

collection at 3 h, 24 h, and 48 h post-EHI. Conceptually it would have been most consistent to allow 0 h EHI mice to rest passively at $25 \pm 2^\circ\text{C}$ for 20 min. However, observations during previous studies and the current one indicate that when removed from heat and placed at 25°C , T_c of EHI mice cools rapidly, and they typically regain consciousness soon thereafter. To compare molecular/cellular events and cytokine levels between EHI versus EHS at the end of their respective heating protocols, EHI mice were euthanized immediately after ending the active heating and EHS mice after removal from 20-min passive heating. There were 15/63 EHS mice that succumbed to premature death (defined as not reaching the designated euthanasia timepoint) due to protocol, and one of the 15 deaths was due to meeting the criteria for humane endpoint. None of the ExC (0/63) and EHI (0/53) animals succumbed to premature death due to protocol.

Blood and Organ Collection

Blood was collected via cardiac puncture, immediately transferred to 500 μL ethylenediaminetetraacetic acid (EDTA)- and 200 μL lithium heparin-coated microcentrifuge tubes, and placed on ice. Aspartate aminotransferase or transaminase (AST), alanine aminotransferase or transaminase (ALT), blood urea nitrogen (BUN), and creatinine (CRE) were determined using a Vetscan VS2 Chemistry Analyzer (Zoetis, Parsippany, NJ). After exsanguination, the liver, kidneys, and heart were excised, rinsed with cold 0.9% saline, snap-frozen in liquid nitrogen, and stored at -80°C .

Plasma Cytokine and Chemokine Measurements

Plasma was separated by centrifugation (4°C ; 10 min, 1,000 g) and stored at -80°C until analysis. Cytokines measured were interleukins-1 β (IL-1 β), -6 (IL-6), -10 (IL-10), and -12 subunit p40 (IL-12p40), granulocyte colony-stimulating factor (G-CSF), and tumor necrosis factor- α (TNF- α). Chemokines measured were interferon γ -induced protein 10 (IP-10, also known as CXCL10), keratinocytes-derived chemokine (KC, also known as CXCL1), macrophage inflammatory proteins 1- α (MIP-1 α , also known as CCL3), 1- β (MIP-1 β , also known as CCL4), and 2 (MIP-2, also known as CXCL2), and regulated on activation, normal T cell expressed and secreted (RANTES, also known as CCL5). All cytokines and chemokines were determined using a MILLIPLEX MAP Mouse Cytokine/Chemokine Panel 12-Plex (Millipore, Burlington, MA) on a Bio-Plex 200 system (Bio-Rad, Hercules, CA) according to the manufacturer's instructions. Sample size was 10–14 mice/group.

Western Blotting

Organs were homogenized in modified tissue protein extraction reagent (T-PER; Thermo Fisher, Waltham, MA) supplemented with 0.2 M sodium vanadate, 0.5 M EDTA, 0.05 M EGTA, 0.1 M sodium pyrophosphate, 0.1 M β -glycerophosphate, 0.1 M phenyl-methyl sulfonyl fluoride, 1 mg/mL leupeptin, and PhosSTOP tablet(s) (Sigma-Aldrich, St. Louis, MO) added. Samples were solubilized with shaking (1 h, 4°C) and separated by centrifugation (15,000 rpm, 15 min, 4°C). Equal amounts of lysate protein concentration were determined using bicinchoninic acid (BCA) assay. Samples were

boiled at 95°C, separated by SDS-PAGE, and transferred to polyvinylidene difluoride membranes overnight at 4°C. Equal loading was confirmed using MemCode protein stain (Thermo Fisher). Membranes were blocked and incubated with appropriate concentrations of primary (1:1,000) and secondary antibodies (1:10,000). Fluorescence imaging (LI-COR Odyssey, Lincoln, NE) was used to visualize protein bands and quantitated via densitometry on ImageJ (NIH, Bethesda, MD). Results were expressed as bands normalized to Memcode staining on the blot. Primary antibodies were directed against heat shock protein at 70 kDa (HSP70; ADI-SPA-812, Enzo Life Sciences, Farmingdale, NY), c-Jun NH₂-terminal kinase (JNK; Cell Signaling Technology, Danvers, MA; 9252 and 4668), nuclear factor- κ B p65 subunit (NF- κ B p65; CST 8242 and 3033), and p38 mitogen-activated protein kinase (MAPK; CST 9212 and 4511). Secondary antibody was LI-COR donkey anti-rabbit 926–32213.

Calculations

Percent dehydration and thermal load were calculated as previously described (26). Thermal load was measured by calculating the area above $T_C = 37.5^\circ\text{C}$ as this was equivalent to T_{Env} , and the assumption was that any temperature above this was due to the onset of hyperthermia. T_{CMax} and T_{Cmin} were the maximum and minimum T_C observed, respectively. Hypothermia duration was defined as the total time where $T_C < 34.5^\circ\text{C}$.

Statistical Analysis

Adequacy of group sizes was determined using a two-sample *t* test power calculation estimating $\sim 1^\circ\text{C}$ reduction in post-EHS hypothermia and accounting for $\sim 30\%$ attrition due to mortality or technical issues with telemeters. With the study design, and roughly 120 observations per biomarker, we had 80% statistical power to detect an ANOVA interaction effect equivalent to Cohen's $f = .35$ (6 numerator, and 108 denominator degrees of freedom), and an effect of Cohen's $d = 0.5$ for pairwise comparisons using the estimated marginal means. All analyses were completed using the R statistical computing language (v. 4.1.2). Thermoregulatory variables were compared using a Wilcoxon rank sum test (EHI vs. EHS) or Kruskal–Wallis test (EHI vs. EHS vs. ExC). For biomarker and cytokine/chemokine analyses, due to significant skew of the distributions (visually confirmed through plots of the residuals), many values were transformed (Box-Cox transformation) to normalize distributions, and the residuals were visually inspected to confirm appropriate model fit. Biomarker comparisons were then made using a linear mixed model with the “lmerTest” R package. For Western blot analysis, comparisons were made using a one-way ANCOVA (total protein as a covariate). Plots are displayed as the estimated marginal means (middle bar) and 95% confidence intervals (bottom and top bars). Comparisons among EHS, EHI, and ExC conditions were made with specific contrasts using the “emmeans” R package. To control for multiple comparisons, a Holm–Bonferroni correction was applied to the pairwise comparisons. Data are expressed as means \pm SD, unless otherwise indicated.

RESULTS

Thermal Data

Values are presented as median [interquartile range (IQR)]. T_{CMax} was elevated in EHS versus EHI mice (42.5°C vs. 42.4°C , $n = 54$ – 63 ; Fig. 1C and Table 1, $P = 0.007$). Thermal load was also higher in EHS versus EHI mice (773 vs. 659 , $n = 38$ – 40 ; Table 1, $P = 0.002$). T_{Cmin} was lower in EHS compared with EHI mice (31.1°C vs. 32.4°C , $n = 21$ – 27 ; Table 1, $P < 0.001$). Duration of hypothermia ($T_C < 34.5^\circ\text{C}$) was longer in EHS versus EHI mice (295 min vs. 206 min, $n = 21$ – 27 ; Table 1, $P < 0.001$). Thermal comparisons were confined to EHS versus EHI mice as all ExC mice had relatively stable T_C throughout the study within a much narrower range than EHS and EHI mice (Fig. 1C). All EHS mice survived exertional heating, but mortality in a subset occurred at some point either during or after passive heating.

Blood Biomarkers

ALT.

ALT in EHS mice was elevated versus ExC at 3 h ($P = 0.008$; $n = 5$ – 10), 24 h ($P < 0.001$; $n = 8$ – 9), and 48 h ($P < 0.001$; $n = 10$ – 12 /group) and versus EHI mice at 48 h ($P = 0.011$; $n = 10$ – 12 /group) (Fig. 2A).

AST.

AST in EHS mice was elevated versus ExC at 3 h ($P < 0.001$; $n = 5$ – 9 /group) and 24 h ($P < 0.001$; $n = 8$ /group) and versus EHI mice at 24 h ($P = 0.015$; $n = 8$ – 11 /group) and 48 h ($P = 0.049$; $n = 10$ – 12 /group) (Fig. 2B).

BUN.

BUN in EHS mice was elevated versus ExC at 0 h ($P < 0.001$; $n = 11$ /group), 3 h ($P < 0.001$; $n = 6$ – 10 /group), and 24 h ($P = 0.005$; $n = 9$ /group) and versus EHI mice at 3 h ($P = 0.005$; $n = 6$ – 13 /group) and 24 h ($P < 0.001$; $n = 9$ – 11 /group) (Fig. 2C).

CRE.

CRE in EHS mice was elevated across all time points (i.e., no time by group interaction; $P = 0.255$) versus ExC and EHI (Fig. 2D).

Chemokines

MIP-1 α /CCL3.

At 3 h, MIP-1 α was elevated in EHS mice versus ExC ($P = 0.007$; $n = 10$ – 12 /group) and EHI mice ($P = 0.016$; $n = 12$ /group) (Fig. 3A).

MIP-1 β /CCL4.

MIP-1 β was elevated in EHS mice versus ExC at 0 h ($P = 0.015$; $n = 10$ – 12 /group) and 3 h ($P < 0.001$; $n = 10$ – 12 /group) and versus EHI mice at 3 h ($P < 0.001$; $n = 12$ /group) (Fig. 3B).

RANTES/CCL5.

RANTES was elevated in EHS mice across all time points (i.e., no time by group interaction; $P = 0.247$) versus ExC and EHI (Fig. 3C).

Table 1. Thermoregulatory responses of EHS mice during heat exposure and recovery

	EHI	EHS	P Value
Heat exposure			
Time to collapse, min	249 (228, 273) (n = 54)	244 (216, 280) (n = 63)	0.9
T _C at collapse, °C	42.3 (42.2, 42.4) (n = 54)	42.3 (42.1, 42.4) (n = 63)	>0.9
T _{CMax} , °C	42.4 (42.2, 42.5) (n = 54)	42.5 (42.3, 42.8) (n = 63)*	0.007
Thermal load, °C·min	659 (593, 755) (n = 40)	773 (653, 889) (n = 38)*	0.002
Dehydration, %	12.4 (11.3, 13.6) (n = 54)	12.7 (11.6, 14.3) (n = 62)	0.3
Recovery			
Time to T _{CMin} , min	121 (106, 141) (n = 27)	135 (122, 179) (n = 21)*	0.031
T _{CMin} , °C	32.4 (32.0, 33.2) (n = 27)	31.1 (29.7, 31.5) (n = 21)*	<0.001
Hypothermia duration, min	206 (178, 243) (n = 27)	295 (250, 464) (n = 19)*	<0.001
Survival, %	100.0	77.4	0.001

Values are median (IQR). **P* < 0.05 compared to EHI with Wilcoxon sum rank test. As ExC mice did not exhibit the thermal fluctuations observed in EHI and EHS mice, they are excluded from the table. Although the time to collapse and T_C at collapse did not differ between EHI vs. EHS mice, T_{CMax} and thermal load were higher in EHS mice, T_{CMin} was lower in EHS mice, and hypothermia duration was longer in EHS mice. EHS mice were also the only group that exhibited mortality due to conditions. ExC, exercise control; EHI, exertional heat injury; EHS, exertional heat stroke; IQR, interquartile range.

IP-10/CXCL10.

IP-10 was elevated in EHS mice versus ExC at 0 h (*P* < 0.001; *n* = 10–12), 3 h (*P* < 0.001; *n* = 10–12), and 24 h (*P* < 0.001; *n* = 10–11) and versus EHI mice at 3 h (*P* < 0.001; *n* = 12/group) and 24 h (*P* < 0.001; *n* = 11/group) (Fig. 3D).

KC/CXCL1.

KC was elevated in EHS mice versus ExC at 3 h (*P* < 0.001; *n* = 10–12/group) and 24 h (*P* < 0.001; *n* = 10–11/group) and versus EHI mice at 3 h (*P* < 0.001; *n* = 12/group) (Fig. 3E).

MIP-2/CXCL2.

MIP-2 was elevated in EHS mice versus ExC at 3 h (*P* < 0.001; *n* = 10–12/group) and 24 h (*P* = 0.029; *n* = 10–11/group) and versus EHI mice at 3 h (*P* < 0.001; *n* = 12/group) (Fig. 3F).

Cytokines

IL-6.

IL-6 in EHS mice was elevated versus ExC at 3 h (*P* < 0.001; *n* = 10–12/group) and 24 h (*P* = 0.011; *n* = 10–11/group) and versus EHI mice at 3 h (*P* < 0.001; *n* = 12/group) and 24 h (*P* = 0.042; *n* = 11/group) (Fig. 4A).

IL-10.

At 3 h, IL-10 was elevated in EHS mice versus ExC (*P* < 0.001; *n* = 9–12/group) and versus EHI mice (*P* = 0.008; *n* = 12/group) (Fig. 4B).

TNF-α.

TNF-α was elevated in EHS mice across all time points (i.e., no time by group interaction; *P* = 0.5) versus ExC and EHI (Fig. 4C).

G-CSF.

G-CSF was elevated in EHS mice versus ExC at 3 h (*P* < 0.001; *n* = 10–12/group) and 24 h (*P* < 0.001; *n* = 10–11/group) and versus EHI mice at 24 h (*P* < 0.001; *n* = 10–11/group) (Fig. 4D).

IL-1β and IL-12p40.

There were no differences in levels of IL-1β or IL-12p40 at any of the time points when comparing ExC or EHI versus EHS (data not shown).

Western Blotting

All Western blot signals were normalized to total protein stains on the same membrane.

Liver.

JNK. Hepatic c-Jun NH₂-terminal kinase (JNK or stress-activated protein kinase – SAPK) was phosphorylated on threonine 183/tyrosine 185 at 0 h in a manner that reflected heat illness severity: EHS > EHI & ExC (*P* < 0.001; *n* = 9 or 10 mice/group; Fig. 5, A and B). However, plots examining the relationship between T_{CMax} or ascending thermal area (aTA) versus phospho-JNK indicated no direct correlation between T_{C/aTA} and JNK phosphorylation in mouse liver at 0 h following EHI and EHS (data not shown).

NF-κβ p65. Nuclear factor-κβ (NF-κβ) p65 subunit phosphorylation on serine 536 was decreased with heat exposure at 0 h in the liver (Fig. 5, C and D); EHI and EHS < ExC (*P* < 0.001 for both comparisons; *n* = 9–10/group), and EHS < EHI (*P* = 0.047; *n* = 9–10/group).

p38 MAPK. p38 MAPK phosphorylation on threonine 180/tyrosine 182 was decreased with heat exposure at 0 h in the liver (Fig. 5, E and F); EHS < ExC (*P* < 0.001; *n* = 9–10/group) with a trend (*P* = 0.053; *n* = 9–10/group) between EHS (0.161 ± 0.021) versus EHI (0.228 ± 0.025).

HSP70. Hepatic heat shock protein at 70 kD (HSP70) was increased with heat exposure at 24 h (Fig. 5, G and H); EHS > EHI and ExC.

Heart.

JNK. For JNK phosphorylation in the heart at 0 h, EHS > ExC (*P* = 0.009; *n* = 7–10 animals/group), but there was no difference between EHS versus EHI (Fig. 6, A and B).

NF-κβ. Heat exposure decreased cardiac NF-κβ p65 phosphorylation at 0 h as EHS < ExC (*P* < 0.001; *n* = 9–10/group), but there was no difference between EHS versus EHI (Fig. 6, C and D).

p38 MAPK. There was no difference between groups for cardiac p38 MAPK phosphorylation (Fig. 6, E and F).

HSP70. Cardiac HSP70 was increased at 24 h following heat exposure: EHS > EHI and ExC (*P* < 0.001 for both comparisons; *n* = 9–10/group; Fig. 6, G and H).

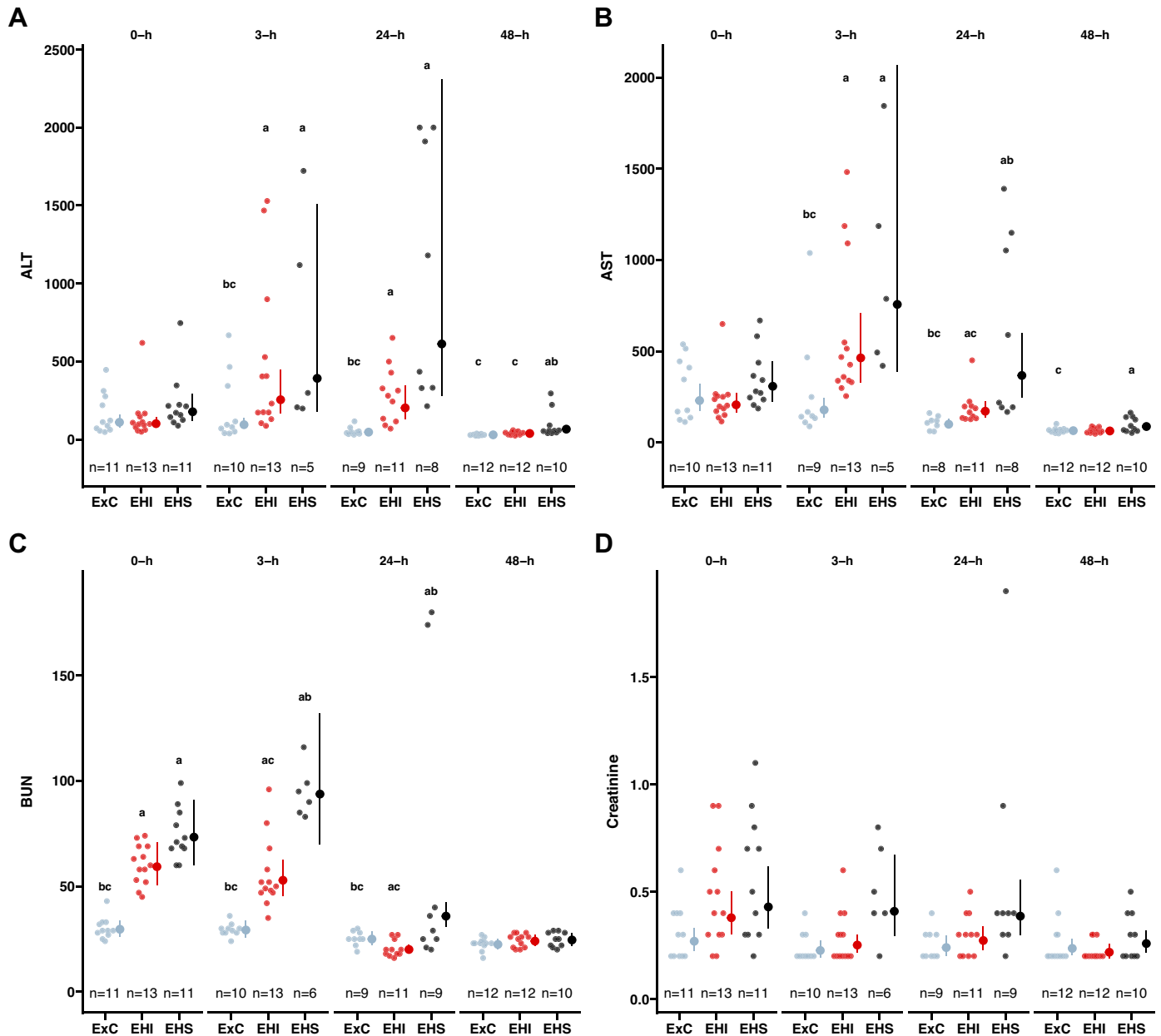


Figure 2. Blood ALT, AST, BUN, and Cre. **A:** ALT was elevated in EHS vs. ExC mice at 3 h ($P < 0.001$; $n = 5-10$ /group), 24 h ($P < 0.001$; $n = 8-9$ /group), and 48 h ($P = 0.008$; $n = 10-12$ /group), in EHS vs. EHI at 48 h ($P = 0.011$; $n = 10-12$ /group), and in EHI vs. ExC mice at 3 h ($P = 0.008$; $n = 9-11$ /group). **B:** AST was elevated in EHS vs. ExC mice at 3 h and 24 h ($P < 0.001$ at both times; $n = 5-9$ /group), in EHS vs. EHI at 24 h ($P = 0.015$; $n = 8-11$ /group) and 48 h ($P = 0.049$; $n = 10-12$ /group), and in EHI vs. ExC at 3 h ($P < 0.001$; $n = 9-13$ /group) and 24 h ($P = 0.017$; $n = 8-11$ /group). **C:** BUN was elevated in EHS vs. ExC at 0 h, 3 h ($P < 0.001$ at both times; $n = 6-11$ /group), and 24 h ($P = 0.005$; $n = 9$ /group), in EHS vs. EHI at 3 h ($P = 0.005$; $n = 6-13$ /group) and 24 h ($P < 0.001$; $n = 9-11$ /group), and in EHI vs. ExC at 0 h and 3 h ($P < 0.001$ at both times; $n = 10-13$ /group). **D:** Cre was elevated in EHS vs. ExC mice at 3 h ($P = 0.02$; $n = 6-10$ /group). BUN and Cre are indicative of renal damage and tended to be elevated more proximal to the onset of EHS but had returned to baseline levels at 24 h and 48 h. In contrast, ALT and AST, which are indicative of hepatic damage, tended to be elevated starting at 3 h and remained elevated through 24 h and 48 h. Consequently, we infer that renal dysfunction/damage precedes liver dysfunction or damage. However, the data also indicate renal dysfunction/damage resolves within 24 h while hepatic damage persists to later timepoints. ^aDifference from ExC, ^bdifferences from EHI, ^cdifference from EHS. ALT, alanine aminotransferase or transaminase; AST, aspartate aminotransferase or transaminase; BUN, blood urea nitrogen; Cre, creatinine; ExC, exercise control; EHI, exertional heat injury; EHS, exertional heat stroke.

Kidney.

JNK. Renal JNK phosphorylation at 0 h was similar to the liver: EHS > EHI and ExC ($P < 0.001$ for both comparisons; $n = 9$ or 10 mice/group for two proteins; Fig. 7, A and B).

HSP70. Renal HSP70 was increased at 24 h (EHS > ExC; $P < 0.001$; $n = 9$ /group), but there was no difference between EHS versus EHI (Fig. 7, G and H).

NF- κ B p65 and p38 MAPK. No differences were observed across groups for NF- κ B p65 and p38 MAPK phosphorylation (Fig. 7, C-F).

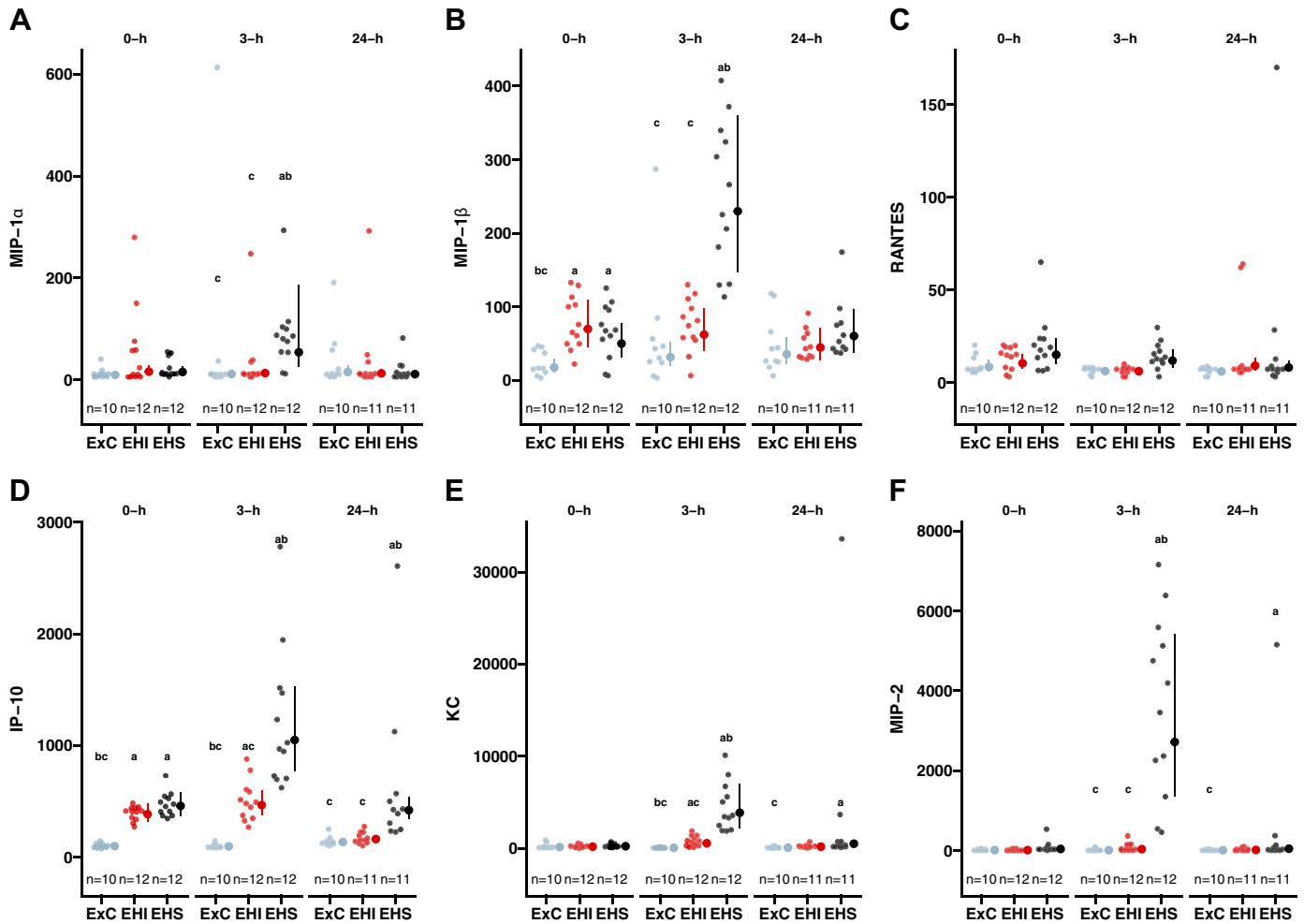


Figure 3. Blood chemokines. **A:** at 3 h, MIP-1 α /CCL3 was elevated in EHS mice vs. ExC ($P = 0.007$; $n = 10$ –12/group) and EHI mice ($P = 0.016$; $n = 12$ /group). **B:** MIP-1 β /CCL4 was elevated in EHS mice vs. ExC at 0 h ($P = 0.015$; $n = 10$ –12/group) and 3 h ($P < 0.001$; $n = 10$ –12/group) and vs. EHI mice at 3 h ($P < 0.001$; $n = 12$ /group). MIP-1 β was also elevated in EHI vs. ExC mice at 0 h ($P < 0.001$; $n = 10$ –12/group). **C:** at 3 h, RANTES/CCL5 was elevated in EHS vs. EHI mice ($P = 0.045$; $n = 12$ /group). **D:** IP-10/CXCL10 was elevated in EHS mice vs. ExC at 0 h, 3 h, and 24 h ($P < 0.001$ at all timepoints; $n = 10$ –12/group) and vs. EHI mice at 3 h and 24 h ($P < 0.001$ at both timepoints; $n = 11$ –12/group). IP-10 was also elevated in EHI vs. ExC mice at 0 h and 3 h ($P < 0.001$ at both times; $n = 10$ –12/group). **E:** KC/CXCL1 was elevated in EHS mice vs. ExC at 3 h and 24 h ($P < 0.001$ at both timepoints; $n = 10$ –12/group) and vs. EHI mice at 3 h ($P < 0.001$; $n = 12$ /group). **F:** MIP-2/CXCL2 was elevated in EHS mice vs. ExC at 3 h ($P < 0.001$; $n = 10$ –12/group) and 24 h ($P = 0.029$; $n = 10$ –11/group) and vs. EHI mice at 3 h ($P < 0.001$; $n = 12$ /group). Chemokines were most elevated in EHS mice at 3 h postheating, possibly indicating the conditions and timing for the most severe inflammatory response. As chemokines control cell migration and positioning in the immune system to induce inflammation, it is likely that mice were experiencing a condition similar to the systemic inflammatory response syndrome (SIRS) at 3 h after EHS. ^aDifference from ExC, ^bdifferences from EHI, ^cdifference from EHS. ExC, exercise control; EHI, exertional heat injury; EHS, exertional heat stroke; KC, keratinocytes-derived chemokine; MIP-1 α , macrophage inflammatory proteins 1- α .

DISCUSSION

The purpose of our current study was to establish a mouse model of EHS more severe than previous iterations of murine exertional heat illnesses and identify therapeutic targets to mitigate EHS effects. An advantage of the current study design was that it enabled the characterization of heat illness gradations (i.e., EHS vs. EHI and ExC) instead of a binary comparison between just EHS and ExC. This allowed us to establish that the difference between EHS and EHI is an exaggerated inflammatory response (i.e., SIRS) in EHS and increased JNK phosphorylation during EHS compared with EHI and ExC. Whether JNK modulates SIRS is yet to be determined.

Establishing an EHS Model

The higher average T_{CMax} in EHS compared with EHI (Fig. 1C and Table 1; individual data in Supplemental Fig. S1A) was due to passive heating of EHS mice after exertional heating/collapse, which resulted in ~23% mortality in EHS mice compared with no deaths in EHI mice (Table 1). In addition, 20 min of passive heating after collapse in EHS mice resulted in lower T_{CMin} and hypothermia duration that was ~150 min longer when compared with EHI mice (Fig. 1C and Table 1; individual data in Supplemental Fig. S1B). The thermal data allow us to conclude that 1) EHS mice exhibited a more severe exertional heat illness phenotype and 2) 20 min of extra heating did not lead to an additive elongation for the

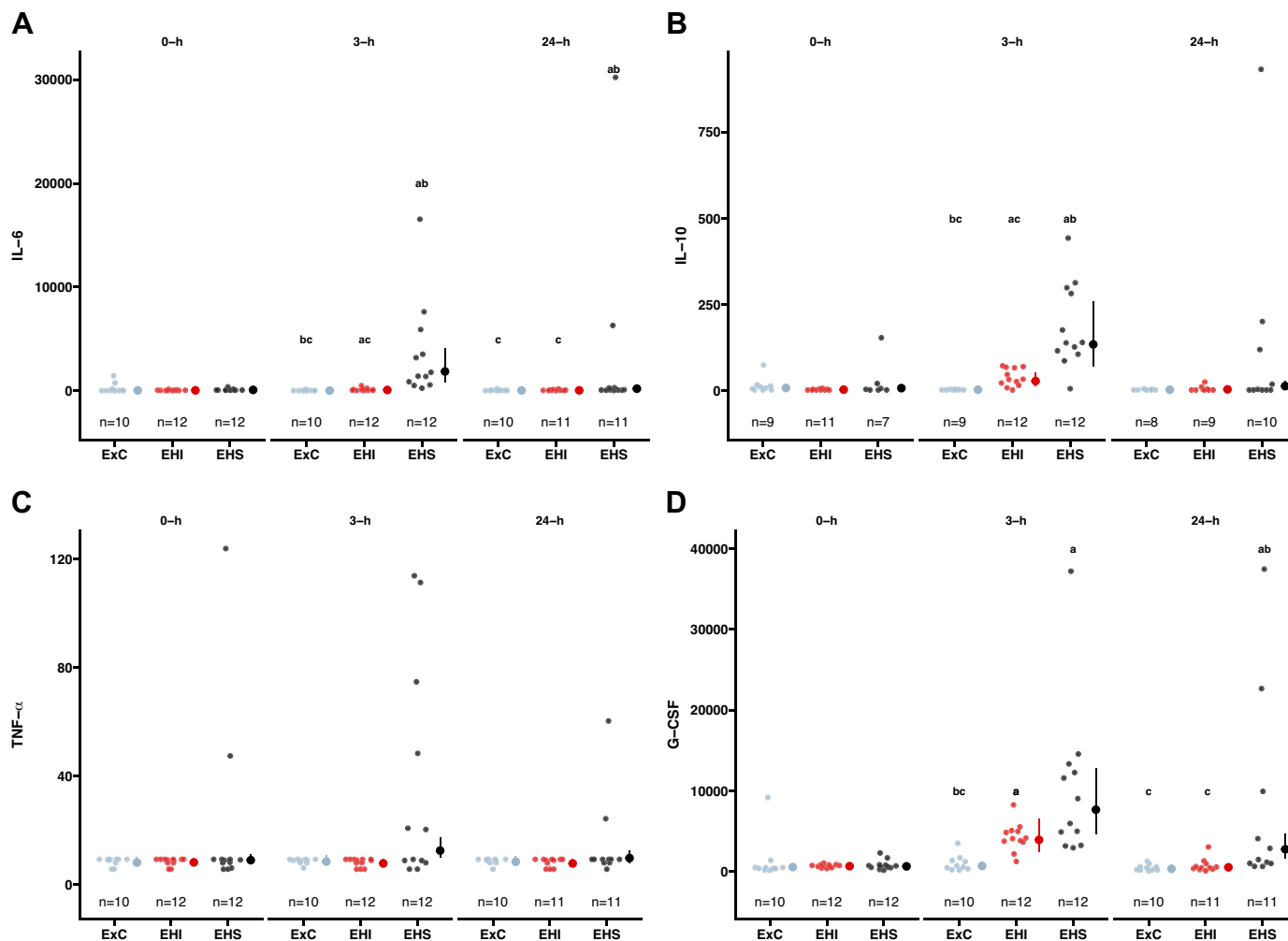


Figure 4. Blood cytokines. **A:** IL-6 in EHS mice was elevated vs. ExC at 3 h ($P < 0.001$; $n = 10$ –12/group) and 24 h ($P = 0.011$; $n = 10$ –11/group) and vs. EHI mice at 3 h ($P < 0.001$; $n = 12$ /group) and 24 h ($P = 0.042$; $n = 11$ /group). IL-6 was also elevated in EHI vs. ExC mice at 3 h ($P = 0.042$; $n = 10$ –12/group). **B:** at 3 h, IL-10 was elevated in EHS mice vs. ExC ($P < 0.001$; $n = 9$ –12/group) and vs. EHI mice ($P = 0.008$; $n = 12$ /group). IL-10 was also elevated in EHI vs. ExC at 3 h ($P < 0.001$; $n = 9$ –12/group). **C:** at 3 h, TNF- α was elevated in EHS vs. EHI mice ($P = 0.022$; $n = 12$ /group). **D:** G-CSF was elevated in EHS mice vs. ExC at 3 h and 24 h ($P < 0.001$ at both timepoints; $n = 10$ –12/group) and vs. EHI mice at 24 h ($P < 0.001$; $n = 11$ /group). G-CSF was also elevated in EHI vs. ExC mice at 3 h ($P < 0.001$; $n = 10$ –12/group). ^aDifference from ExC, ^bdifferences from EHI, ^cdifference from EHS. ExC, exercise control; EHI, exertional heat injury; EHS, exertional heat stroke; G-CSF, granulocyte colony-stimulating factor; IL, interleukin; TNF, tumor necrosis factor.

separate phases of thermal response in EHS compared with EHI mice (i.e., 20 min of passive heating did not simply elongate hypothermia by ~ 20 min). These findings are likely consistent with human cases where the area under the curve for thermal load has a strong positive correlation to EHS severity (28).

EHS mice that died prematurely typically exhibited a pronounced and accelerated T_C rise during the last 10 min of passive heating, occasionally increasing to $\geq 43^\circ\text{C}$ (Supplemental Fig. S2). It is unknown what processes caused the abrupt T_C rise, but as this often occurred during passive heating, premature EHS deaths typically occurred closer to the end of heating or 0 h than the 3-h time point. The possibility of prolonged heat exposure and dehydration contributing to renal damage has been suggested in a mouse model of Mesoamerican nephropathy (29). Although dehydration and water restriction during running + heating could have contributed to organ damage in EHS and EHI mice relative to

ExC in the current study, percent dehydration was not different between EHS and EHI groups (Table 1) and did not correspond to EHS severity. Even after accounting for water consumed the night before testing, there was still no correspondence between dehydration and EHS severity. Although weight loss is not particularly sensitive to just water loss, and mice could have also lost mass through energy expenditure and defecation, these limitations are encountered by others when quantifying dehydration (30). Analyses of mouse body weights, in-cage activity, and T_C before heating were also not predictive of which mice would experience more or less severe EHS (data not shown).

Characterization of the Differences in the Magnitude and Temporal Pattern of Biomarkers with EHI versus EHS

The circulating biomarkers examined in the current study indicate organ damage occurrence and are affected during

liver dysfunction/damage is delayed, hepatic issues are more extensive, requiring a longer recovery duration. This interpretation is consistent with conclusions drawn from a retrospective human study (34) and aligns with clinical reports indicating elevated liver biomarkers occur relatively late (2–3 days) following EHS onset in patients (32, 35). Our biomarker results in EHS mice indicate temporal aspects of their pathophysiology may parallel the sequence of events in human EHS cases. Consequently, the EHS model we have established is not only more severe than previous iterations of murine exertional heat illness but could also be better suited to identify EHS-related cellular/molecular events in humans.

For the current study, we measured the CC motif ligand (CCL) and the CXC motif ligand (CXCL) chemokines, which control coordinated cell migration and cell positioning throughout development, homeostasis, and inflammation (36). At 3 h postheating, most of the cytokines/chemokines investigated tended to be elevated to peak levels in EHS mice, above levels measured in ExC and/or EHI mice (Fig. 4 and Fig. 5). The 3-h timepoint also roughly corresponds to hypothermia (<34.5°C) and/or T_{CMin} (lowest recorded T_C during protocol; Fig. 1C, Fig. 3, and Fig. 4). Of the cytokines/chemokines quantitated, the pattern of IP-10 (CXCL10; Fig. 3D) corresponded most closely with gradations of heat illness severity. IP-10 levels peaked at 3 h in EHS mice, and this is consistent with previous observations of IP-10 in murine exertional heat illness (21). At 24 h, IP-10 was still elevated in EHS mice while it had returned to basal levels in EHI mice. Transient IP-10 elevations are typically associated with acute damage to tissues or organs such as neural tissue following cerebral ischemia (37) or possibly heat stress in hepatocytes (38). IP-10 acts as a chemoattractant for monocytes and T cells (39), initiating an *in vivo* immune response (40), and elicits multiple biological responses including the chemotactic activity of cells to induce apoptosis, regulating cell growth/proliferation and angiogenesis in infectious/inflammatory diseases (41). KC and MIP-2, also CXCL chemokines, were both elevated in EHS compared with EHI at 3 h and in EHS compared with ExC at 3 h and 24 h (Fig. 3, E and F), exhibiting nearly identical fluctuation patterns. In contrast to CXCL chemokines, CCL chemokines—MIP-1 α , MIP-1 β , and RANTES (Fig. 3, A–C)—and the cytokines (Fig. 4) did not exhibit a uniform pattern of fluctuations aside from all of them reaching peak levels at 3 h in EHS mice. The overall pattern of cytokines at 3 h (Fig. 4 and Fig. 5) inversely corresponded/correlated to T_C of tested mice (Fig. 1C). EHS mice exhibited higher cytokine levels and lower T_{CMin} compared with EHI mice; ExC mice did not exhibit any cytokine/chemokine elevations or hypothermia. These cytokines/chemokines

could be regulating or reflecting heat illness severity considering they follow a similar pattern to the liver (ALT and AST) and kidney (BUN and CRE) biomarkers (Fig. 2).

Western Blotting Identified Proteins Potentially Involved in Modulating EHS Severity

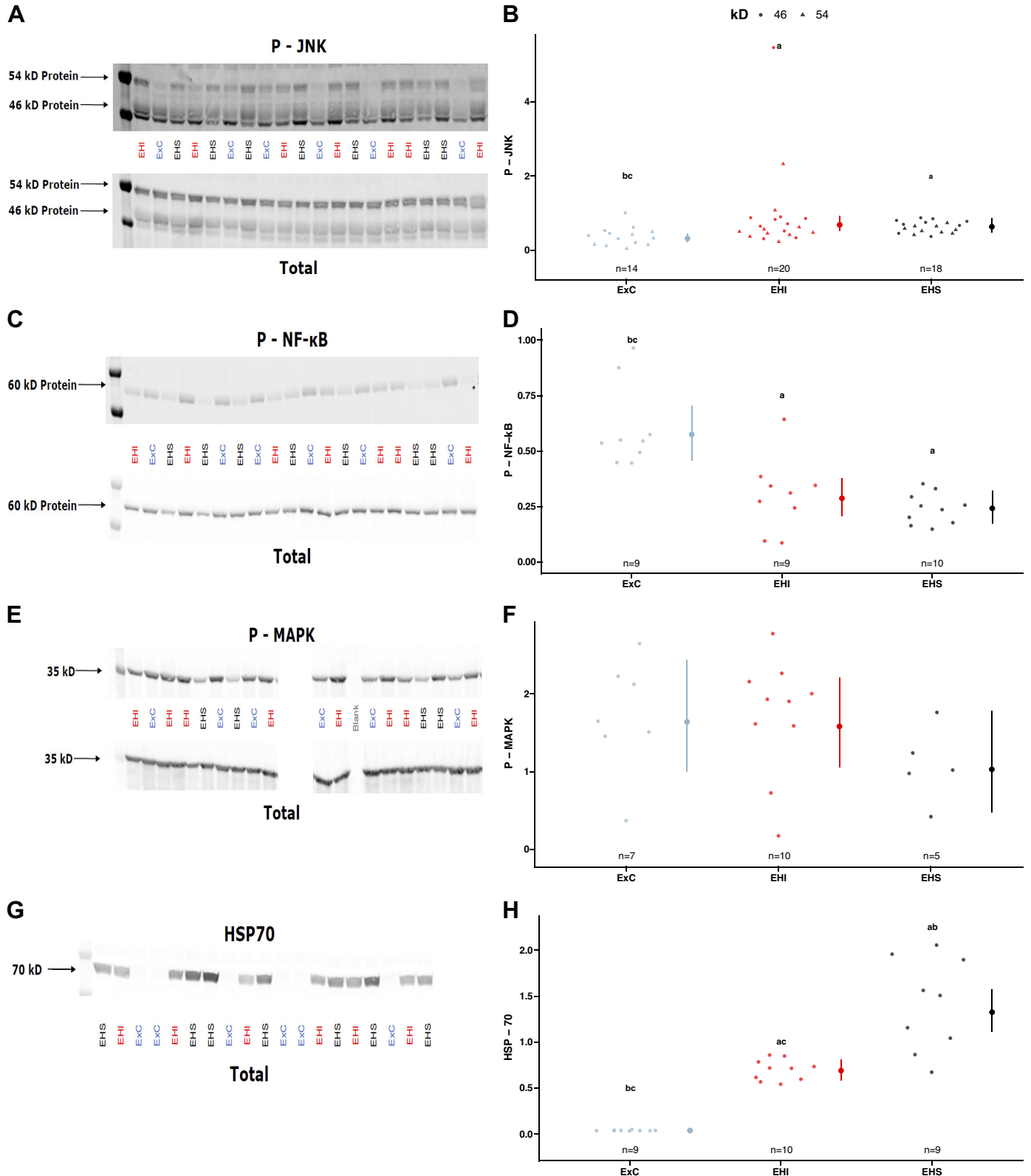
Heating increased HSP70 in liver, heart, and kidneys at 24 h (Fig. 5, G and H; Fig. 6, G and H; and Fig. 7, G and H). The liver and the heart exhibited a gradient in HSP70 where EHS was greater than EHI with the lowest levels in ExC (Fig. 5, G and H; Fig. 6, G and H). We have previously reported that mice experiencing two consecutive EHIs separated by 1–7D required longer running time and heat exposure to induce the second EHI, suggestive of enhanced heat tolerance with successive EHI bouts. Those mice also displayed higher T_{CMax} and T_{CMin} and spent less time below resting T_C (~36.5°C), suggesting that increased HSP70 may underlie heat tolerance (26). However, despite the potential benefits of elevated HSP70 on heat tolerance during heat illnesses, an alternative perspective is that HSP70 levels may be proportional to or indicative of the extent of heat-induced organ damage suffered 24 h prior. As HSP70 is a chaperone protein recruited to remove damaged proteins and promote cell survival following exposure to a stressor, the greatest HSP70 levels likely reflect the most serious heat and/or inflammatory damage in our model. Measuring HSP70 as a diagnostic marker for stress or toxin exposure has previously been proposed by teams investigating other conditions (42, 43).

Most premature EHS deaths occurred closer to 0 h, although ~3 h after collapse from EHI/EHS is when cytokines and chemokines were elevated to peak levels and exhibit the most robust differences compared with thermoneutral exercise. This led us to infer that events closer to collapse possibly preceding cytokine/chemokine elevations at 3 h may have led to death, and we were interested in characterizing fast-response, posttranslational protein modifications at 0 h. We examined protein phosphorylation in organs responsive to heating in EHI/EHS mice and postulated that 0 h activation of signaling proteins could serve as markers for the gradation of heat illness severity and underlie cytokine elevations. A kinase implicated in underlying responses to multiple stressors, including heat, is JNK (also known as stress-activated protein kinase or SAPK in some studies). JNK is a member of the MAPK family of stress response kinases, containing phosphorylation motifs at threonine (Thr) 183/tyrosine (Tyr) 185, which are putative activation sites (44). Activated JNK phosphorylates downstream targets such as c-Jun/AP-1 on multiple phosphorylation motifs (45–47) to induce cellular responses in various tissues/organs (48). We examined JNK phosphorylation in organs particularly vulnerable to EHS

Figure 5. Hepatic proteins. At 0 h in the liver: A and B: JNK was not phosphorylated in response to exercise alone at 25°C. However, JNK was phosphorylated in response to EHS and EHI conditions at 54 and 46 kDa with EHS having greater phosphorylation levels than EHI and ExC (EHS > EHI and ExC; $P < 0.001$ for both), and EHI having greater phosphorylation levels than ExC (EHI > ExC; $P < 0.001$). Assessment of total protein levels indicated no difference across groups. C and D: NF- $\kappa\beta$ was most strongly phosphorylated in ExC mice but was not phosphorylated in EHI and EHS (EHS and EHI < ExC, $P < 0.001$ for both) mice. There was also a difference between EHI and EHS (EHS < EHI; $P = 0.047$). There were no differences in total protein levels across all groups. E and F: p38 MAPK exhibited a similar pattern as NF- $\kappa\beta$ with highest phosphorylation in ExC, lower phosphorylation in EHI and EHS with no differences between the heated groups (EHS and EHI < ExC; $P < 0.001$), and no significant differences in total protein levels. G and H: at 24 h in the liver, HSP70 showed a pattern where EHS > EHI ($P = 0.003$) and ExC ($P < 0.001$) and EHI > ExC ($P < 0.001$). Loading for each blot was normalized to Memcode-detected total protein levels. ^aDifference from ExC, ^bdifferences from EHI, ^cdifference from EHS. ExC, exercise control; EHI, exertional heat injury; EHS, exertional heat stroke; HSP70, heat shock protein at 70 kDa; JNK, c-Jun NH2-terminal kinase; NF- $\kappa\beta$, nuclear factor $\kappa\beta$; MAPK, mitogen-activated protein kinase.

damage: the liver, heart, and kidneys (17). EHS mice subjected to the most severe conditions had the strongest signal for JNK phosphorylation at 0 h in the liver and kidney. JNK phosphorylation pattern was also observed to follow

the gradient for heat illness severity; stronger in EHS compared with EHI with little to no activation in ExC for the long-form and short-form of the protein at 54 kDa and 46 kDa, respectively (Fig. 5, A and B and Fig. 7, A and B).



Accordingly, we infer that JNK phosphorylation in the liver and kidneys may contribute to EHS pathophysiology, and levels of hepatic and renal JNK phosphorylation may mediate or reflect heat illness severity.

With our current study design, it is difficult to discern whether increased JNK phosphorylation initiates/mediates heat illness onset, or whether it signifies a detrimental or protective response against hyperthermia and/or inflammation. However, JNK activation is implicated in inducing cell apoptosis and necrosis during excitotoxicity, ischemia, and neurodegeneration (49), is observed with acetaminophen-associated hepatotoxicity in mice (50, 51), and evidence from a cell culture model suggests that inhibition of JNK dephosphorylation may underlie severity of heat stress effects (52). Accordingly, JNK phosphorylation may underlie EHS severity, and this raises the question of whether JNK inhibition could decrease EHS severity and improve patient/subject outcomes. To our knowledge, this question has not been directly resolved in humans or animals suffering EHS, although several studies have examined JNK inhibition in other models of hepatic toxicity and damage. In mice, the JNK inhibitor SP600125 mitigates acetaminophen-induced hepatocyte necrosis and rises in serum ALT levels at 24 h when it is administered within 5 h after acetaminophen (53). Pretreatment of mice with SP600125 1 h before acetaminophen also attenuates serum ALT and mitigates hepatic necrosis as measured by histology at 24 h and prevents mortality at 24–48 h after acetaminophen. However, in vivo JNK inhibition does not confer protection against concanavalin A-induced hepatic damage, indicating JNK inhibition may not be effective for all types of liver injuries (54). Taken together, the findings from this study and previous ones suggest that the therapeutic potential for inhibiting phosphorylation or facilitating de-phosphorylation of JNK and its downstream targets (e.g., c-Jun) after EHS onset requires further investigation. Practical consideration should also be given to whether such interventions would be better suited for prophylaxis (prevention/delaying onset) or post-EHS primary/supportive treatment. As the current and previous work have indicated mice cool rapidly upon removal from heat (21, 23, 26), but there can still be mortalities in spite of rapid cooling (Table 1, Supplemental Fig. S2), JNK inhibition could still have a robust effect in mice when administered proximal to heat collapse. However, it is uncertain how this would translate to human cases, where patients do not cool as rapidly as mice upon removal from a warm environment following heat collapse (28). Consequently, it is best to immerse human patients in circulating cold water per current guidelines (7). Perhaps JNK inhibition could be used in conjunction with cooling when organ damage is severe or liver transplantation is being considered, but further testing is required.

NF- κ B is another protein implicated in several stress-response pathways related to heat, exercise, and endotoxin; heat stroke may be exacerbated by endotoxin in humans (55) and primates (56, 57). NF- κ B p65 is downstream of and activated in response to endotoxin binding TLR4 in various organs (58). Our data indicate heat stress either prevents phosphorylation or dephosphorylates/facilitates de-phosphorylation of serine (Ser) 536 in the liver and heart; Ser536 phosphorylation was lowest in EHS and EHI (no difference between groups) and greatest in ExC. Furthermore, total levels of NF- κ B p65 were similar across all compared groups in the liver and heart (Figs 5, C and D and Fig. 6, C and D). Our findings are consistent with what others have observed (59, 60) or postulated (25). Preventing phosphorylation of NF- κ B p65 at amino acid 536 by knock-in (KI) substitution of serine to alanine in mice leads to increased mortality of KI specimens relative to wild type (WT) after endotoxin treatment (59). Analysis of methylation in the cardiac genome of EHS mice indicated repression of NF- κ B transcription products, which led Murray et al. (25) in their study to conclude heat exposure represses NF- κ B and its action in the heart. However, Murray et al. (25) in their study confined their observations to female mice whereas our measurements were made exclusively in male mice, and in their model, females experience more severe cardiac symptoms than males (61). Consequently, it is uncertain whether their findings would be identical to ours, although the findings from their work and ours converge on the possibility that NF- κ B may contribute to EHS symptoms. In addition, complete knockout (KO) of NF- κ B p65 in mice is embryonic lethal with extensive liver damage in KO compared with WT littermate fetuses (60). Taken together, hyperthermia disrupts NF- κ B p65 Ser536 phosphorylation, and this could induce apoptosis in affected organs, potentially causing detrimental hepatic and cardiac effects.

Similar to JNK, p38 MAPK is a member of the MAPK family with dual phosphorylation on threonine/tyrosine motifs (at amino acids 180 and 182, respectively). However, the two kinases may antagonize each other in hepatocytes during development, adulthood, and damage/regeneration processes (62). In contrast to JNK, p38 MAPK phosphorylation in liver was greatest in ExC and decreased after heat exposure with no difference between EHS compared with EHI (Fig. 5, E and F). We did not observe differences in p38 MAPK phosphorylation in kidneys and heart. The results suggest that p38 MAPK in the liver may be important in regulating heat illness pathology, and hepatic p38 MAPK is likely constitutively phosphorylated in nonpathological states. The latter is consistent with previous findings where hepatic p38 MAPK is phosphorylated under control conditions and dephosphorylated after cell stress or trauma induced by chemical treatment or injury (63, 64). Consequently, hyperthermia may

Figure 6. Cardiac proteins. At 0 h in the heart: A and B: EHS > ExC ($P = 0.009$) and EHI > ExC ($P = 0.005$) for JNK phosphorylation with no differences between EHS and EHI. There were no differences in total JNK. C and D: EHS < ExC ($P < 0.001$) and EHI < ExC ($P = 0.001$) for NF- κ B p65 phosphorylation while there were no differences between EHS and EHI, and total levels were equal across conditions. E and F: There were no differences across EHS vs. EHI, EHS vs. ExC, or EHI vs. ExC for p38 MAPK phosphorylation ($n = 5$ –10/group). Two segments for both blots are taken from the same membrane; gap in the middle is due to an area where samples for a different study were loaded. G and H: At 24 h in the heart, HSP70 was increased at 24 h such that EHS > EHI and ExC and EHI > ExC ($P < 0.001$ for all comparisons). Loading for each blot was normalized to Memcode-detected total protein levels. ^aDifference from ExC, ^bdifferences from EHI, ^cdifference from EHS. ExC, exercise control; EHI, exertional heat injury; EHS, exertional heat stroke; HSP70, heat shock protein at 70 kDa; JNK, c-Jun NH2-terminal kinase; NF- κ B, nuclear factor κ B; MAPK, mitogen-activated protein kinase.

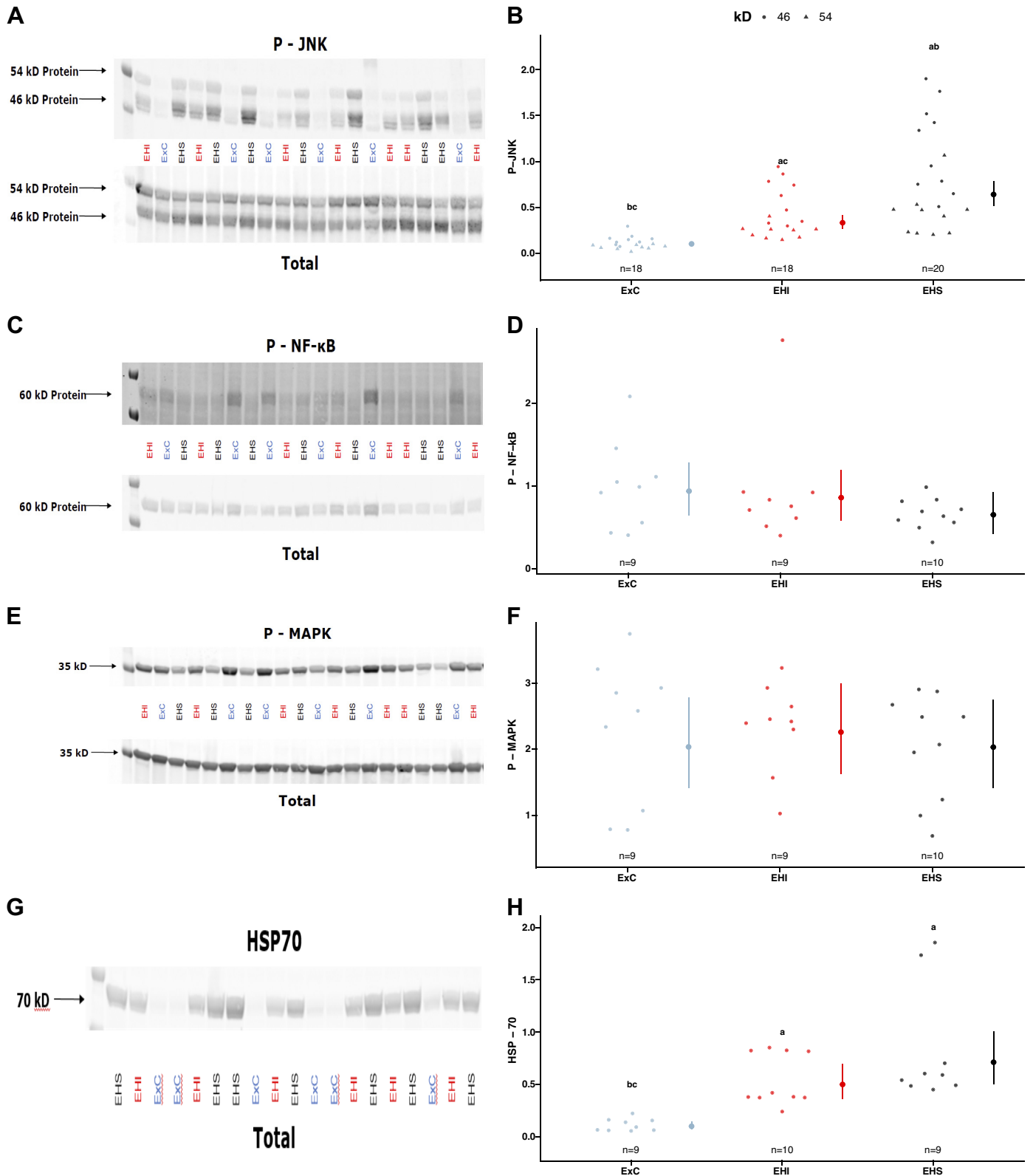


Figure 7. Renal proteins. At 0 h in the kidneys: **A** and **B**: EHS > EHI and ExC and EHI > ExC for JNK phosphorylation ($P < 0.001$ for all comparisons) despite total JNK levels being equal. **C–F**: no differences in phosphorylation were observed across any groups for NF- κ B p65 and p38 MAPK with levels of respective total proteins being equal across all groups. At 24 h (**G** and **H**) HSP70 was increased so that EHS > ExC, and EHI > ExC ($P < 0.001$ for both comparisons), but there were no differences between EHS and EHI. Total protein levels were similar across all groups. ^aDifference from ExC, ^bdifferences from EHI, ^cdifference from EHS. ExC, exercise control; EHI, exertional heat injury; EHS, exertional heat stroke; HSP70, heat shock protein at 70 kDa; JNK, c-Jun NH2-terminal kinase; NF- κ B, nuclear factor κ B; MAPK, mitogen-activated protein kinase.

suppress hepatic p38 MAPK phosphorylation, which could exacerbate cell and organ damage.

Limitations

The extent and pathology of organ damage and cell types affected (e.g., hepatocytes, Kupffer cells, hepatic stellate cells, or liver sinusoidal endothelial cells in liver) during EHS/EHI were not determined via histological analysis. For kinases examined, we did not identify specific isoforms involved during heat- or inflammation-related pathology. Mice have a greater surface area to body mass ratio compared with humans and cool very quickly upon removal from heat. The decrease in T_C in mice is comparable to the cooling rates observed in humans during cold water immersion (7). However, even after regaining consciousness and T_C stabilization, mice still exhibited signs of liver damage for at least 48 h; this suggests additional treatment during post-cooling convalescence may be vital for a full recovery. The current study was conducted examining only male C57BL/6J mice, and we acknowledge that other studies indicate baseline and stress-response physiology differ when comparing 1) C57BL/6J males and females (61, 65), 2) male mice across different strains (66), and 3) different rodent species (67).

PERSPECTIVES AND SIGNIFICANCE

We have refined parameters for a mouse EHS model that may parallel the severity and temporal aspects of cellular/molecular pathophysiology observed in human patients with EHS. The gradation between EHI and EHS in the current study enabled quantitation of what could contribute to lethality and sequelae in EHS. Most EHS mice survived but a subset of specimens died prematurely during or after passive heating. We have identified molecular signaling nodes where (de-)phosphorylation of particular proteins may correspond with more severe heat illness. Specifically, hepatic and renal JNK activation may correspond to heat illness severity. Although clear determination of whether this kinase is harmful or protective during heat illness was not possible with the current study design, evidence linking JNK phosphorylation to hepatotoxicity and hepatocyte apoptosis as well as intervention studies indicating JNK inhibition can attenuate hepatotoxicity/mortalities in animal models lead us to believe JNK is likely involved in organ/tissue damage. It is yet to be determined whether modulating JNK phosphorylation via intervention following heating could affect EHS severity, but this is a possibility we hope to investigate further. Overall, the establishment of a more severe murine EHS model with data on potential mechanism(s) underlying EHS severity will allow for future studies to better understand the inflammatory pathways and proteins involved in EHS-related mortality and test countermeasure options to minimize the damage caused by EHS.

SUPPLEMENTAL DATA

Supplemental Figures S1 and S2: <http://www.doi.org/10.17605/OSF.IO/9FAM3>.

DATA AVAILABILITY

Memcode plots and summaries of the data analysis can be found at Open Science Framework Repository <http://www.doi.org/10.17605/OSF.IO/9FAM3>.

ACKNOWLEDGMENTS

The authors thank the Veterinary Support and Oversight Branch at the United States Army Research Institute of Environmental Medicine for their technical assistance with surgical procedures, animal monitoring, and dissections throughout the study.

GRANTS

This study was supported by the United States Army Medical Research and Development Command (MRDC) to L.R. Leon and in part by appointments to the Department of Defense (DoD) Research Participation Program administered by the Oak Ridge Institute for Science and Education (ORISE) through an inter-agency agreement between the United States Department of Energy (DoE) and the DoD. ORISE is managed by the Oak Ridge Associated Universities (ORAU) under DoE contract number DE-SC0014664.

DISCLOSURES

The opinions or assertions contained herein are the private views of the author(s) and are not to be construed as official or as reflecting the views of the Army, the DoD, the DoE, or ORAU/ORISE. Citations of commercial organizations and trade names in this report do not constitute an official Department of the Army endorsement or approval of the products or services of these organizations. No conflicts of interest, financial or otherwise, are declared by the authors.

AUTHOR CONTRIBUTIONS

K.O., S.M.W., J.A.W., M.L.P., T.A.M., A.R.C., and L.R.L. conceived and designed research; K.O., C.G.H., S.M.W., J.A.W., M.L.P., and T.A.M. performed experiments; K.O., C.G.H., S.M.W., J.A.W., M.L.P., T.A.M., A.R.C., and L.R.L. analyzed data; K.O., C.G.H., S.M.W., J.A.W., M.L.P., T.A.M., A.R.C., and L.R.L. interpreted results of experiments; K.O., C.G.H., S.M.W., J.A.W., M.L.P., A.R.C., and L.R.L. prepared figures; K.O., C.G.H., S.M.W., J.A.W., M.L.P., T.A.M., A.R.C., and L.R.L. drafted manuscript; K.O., C.G.H., S.M.W., J.A.W., M.L.P., T.A.M., A.R.C., and L.R.L. edited and revised manuscript; K.O., C.G.H., S.M.W., J.A.W., M.L.P., T.A.M., A.R.C., and L.R.L. approved final version of manuscript.

REFERENCES

1. Leon LR, Bouchama A. Heat stroke. *Compr Physiol* 5: 611–647, 2015. doi:10.1002/cphy.c140017.
2. Broessner G, Beer R, Franz G, Lackner P, Engelhardt K, Brenneis C, Pfausler B, Schmutzhard E. Case report: severe heat stroke with multiple organ dysfunction - a novel intravascular treatment approach. *Crit Care* 9: R498–R501, 2005. doi:10.1186/cc3771.
3. Yaqub BA, Daif AK, Panayiotopoulos CP. Pancerebellar syndrome in heat stroke: clinical course and CT scan findings. *Neuroradiology* 29: 294–296, 1987. doi:10.1007/BF00451771.
4. Bouchama A, Knochel JP. Heat stroke. *N Engl J Med* 346: 1978–1988, 2002. doi:10.1056/NEJMra011089.
5. Williams VF, Oh GT. Update: Heat illness, active component, U.S. Armed Forces, 2021. *MSMR* 29: 8–14, 2022.

6. **Armed Forces Health Surveillance Branch.** Update: Heat illness, active component, U.S. Armed Forces, 2020. *MSMR* 28: 10–15, 2021.
7. **Casa DJ, DeMartini JK, Bergeron MF, Csillan D, Eichner ER, Lopez RM, Ferrara MS, Miller KC, O'Connor F, Sawka MN, Yeargin SW.** National Athletic Trainers' Association Position Statement: exertional heat illnesses. *J Athl Train* 50: 986–1000, 2015. [Erratum in *J Athl Train* 52: 401, 2017]. doi:10.4085/1062-6050-50.9.07.
8. **Gubernot DM, Anderson GB, Hunting KL.** Characterizing occupational heat-related mortality in the United States, 2000-2010: an analysis using the Census of Fatal Occupational Injuries database. *Am J Ind Med* 58: 203–211, 2015. doi:10.1002/ajim.22381.
9. **Laitano O, Oki K, Leon LR.** The role of skeletal muscles in exertional heat stroke pathophysiology. *Int J Sports Med* 42: 673–681, 2021. doi:10.1055/a-1400-9754.
10. **Department of the Army.** *Technical Bulletin, Medical 507: Heat Stress Control and Heat Casualty Management.* Washington, DC, 2022. https://armypubs.army.mil/epubs/DR_pubs/DR_a/ARN35159-TB_MED_507-000-WEB-1.pdf. [accessed 1 September 2022].
11. **Epstein Y, Yanovich R.** Heatstroke. *N Engl J Med* 380: 2449–2459, 2019. doi:10.1056/NEJMra1810762.
12. **Heneghan HM, Nazirawan F, Dorcaratto D, Fiore B, Boylan JF, Maguire D, Hoti E.** Extreme heatstroke causing fulminant hepatic failure requiring liver transplantation: a case report. *Transplant Proc* 46: 2430–2432, 2014. doi:10.1016/j.transproceed.2013.12.055.
13. **Ichai P, Laurent-Bellue A, Camus C, Moreau D, Boutonnet M, Saliba F, Peron JM, Ichai C, Gregoire E, Aigle L, Cousty J, Quinart A, Pons B, Boudon M, André S, Coilly A, Antonini T, Guettier C, Samuel D.** Liver transplantation in patients with liver failure related to exertional heatstroke. *J Hepatol* 70: 431–439, 2019. doi:10.1016/j.jhep.2018.11.024.
14. **Martinez-Insfran LA, Alconchel F, Ramirez P, Cascales-Campos PA, Carbonell G, Barona L, Pons JA, Sanchez-Bueno F, Robles-Campos R, Parrilla P.** Liver transplantation for fulminant hepatic failure due to heat stroke: a case report. *Transplant Proc* 51: 87–89, 2019. doi:10.1016/j.transproceed.2018.03.137.
15. **Berger J, Hart J, Millis M, Baker AL.** Fulminant hepatic failure from heat stroke requiring liver transplantation. *J Clin Gastroenterol* 30: 429–431, 2000. doi:10.1097/00004836-200006000-00015.
16. **Saïssy JM, Almanza L, Samuel D, Pats B.** [Liver transplantation after exertion-induced heat stroke associated with fulminant liver failure]. *Presse Med* 25: 977–979, 1996.
17. **Wallace RF, Kriebel R, Punnett L, Wegman DH, Amoroso PJ.** Prior heat illness hospitalization and risk of early death. *Environ Res* 104: 290–295, 2007. doi:10.1016/j.envres.2007.01.003.
18. **Ray BR, Pemberton MR, Hourani LL, Witt M, Olmsted KL, Brown JM, Weimer B, Lance ME, Marsden ME, Scheffler S, Vandermaas-Peeler R, Aspinwall KR, Anderson E, Spagnola K, Close K, Gratton JL, Calvin S, Bradshaw M.** *Department of Defense Survey Of Health Related Behaviors Among Active Duty Military Personnel.* RTI International, 2009. <https://apps.dtic.mil/sti/pdfs/ADA527178.pdf>. [accessed 1 September 2022].
19. **Hubbard RW, Bowers WD, Matthew WT, Curtis FC, Criss RE, Sheldon GM, Ratteree JW.** Rat model of acute heatstroke mortality. *J Appl Physiol Respir Environ Exerc Physiol* 42: 809–816, 1977. doi:10.1152/jappl.1977.42.6.809.
20. **King MA, Leon LR, Morse DA, Clanton TL.** Unique cytokine and chemokine responses to exertional heat stroke in mice. *J Appl Physiol (1985)* 122: 296–306, 2017. doi:10.1152/jappphysiol.00667.2016.
21. **King MA, Leon LR, Mustico DL, Haines JM, Clanton TL.** Biomarkers of multiorgan injury in a preclinical model of exertional heat stroke. *J Appl Physiol (1985)* 118: 1207–1220, 2015. doi:10.1152/jappphysiol.01051.2014.
22. **Quinn CM, Duran RM, Audet GN, Charkoudian N, Leon LR.** Cardiovascular and thermoregulatory biomarkers of heat stroke severity in a conscious rat model. *J Appl Physiol (1985)* 117: 971–978, 2014. doi:10.1152/jappphysiol.00365.2014.
23. **Leon LR, DuBose DA, Mason CW.** Heat stress induces a biphasic thermoregulatory response in mice. *Am J Physiol Regul Integr Comp Physiol* 288: R197–R204, 2005. doi:10.1152/ajpregu.00046.2004.
24. **King MA, Alzahrani JM, Clanton TL, Laitano O.** A preclinical model of exertional heat stroke in mice. *J Vis Exp* 173: e62738, 2021. doi:10.3791/62738.
25. **Murray KO, Brant JO, Iwaniec JD, Sheikh LH, de Carvalho L, Garcia CK, Robinson GP, Alzahrani JM, Riva A, Laitano O, Kladdé MP, Clanton TL.** Exertional heat stroke leads to concurrent long-term epigenetic memory, immunosuppression and altered heat shock response in female mice. *J Physiol* 599: 119–141, 2021. doi:10.1113/JP280518.
26. **Caldwell AR, Oki K, Ward SM, Ward JA, Mayer TA, Plamper ML, King MA, Leon LR.** Impact of successive exertional heat injuries on thermoregulatory and systemic inflammatory responses in mice. *J Appl Physiol (1985)* 131: 1469–1485, 2021. doi:10.1152/jappphysiol.00160.2021.
27. **Leon LR, Dineen S, Blaha MD, Rodriguez-Fernandez M, Clarke DC.** Attenuated thermoregulatory, metabolic, and liver acute phase protein response to heat stroke in TNF receptor knockout mice. *Am J Physiol Regul Integr Comp Physiol* 305: R1421–R1432, 2013. doi:10.1152/ajpregu.00127.2013.
28. **Heled Y, Rav-Acha M, Shani Y, Epstein Y, Moran DS.** The “golden hour” for heatstroke treatment. *Mil Med* 169: 184–186, 2004. doi:10.7205/MILMED.169.3.184.
29. **Roncal Jimenez CA, Ishimoto T, Lanaspá MA, Rivard CJ, Nakagawa T, Ejaz AA, Cicerchi C, Inaba S, Le M, Miyazaki M, Glaser J, Correa-Rotter R, González MA, Aragón A, Wesseling C, Sánchez-Lozada LG, Johnson RJ.** Fructokinase activity mediates dehydration-induced renal injury. *Kidney Int* 86: 294–302, 2014. doi:10.1038/ki.2013.492.
30. **Byrne C, Lee JK, Chew SA, Lim CL, Tan EY.** Continuous thermoregulatory responses to mass-participation distance running in heat. *Med Sci Sports Exerc* 38: 803–810, 2006. doi:10.1249/01.mss.0000218134.74238.6a.
31. **Dematte JE, O'Mara K, Buescher J, Whitney CG, Forsythe S, McNamee T, Adiga RB, Ndukwu IM.** Near-fatal heat stroke during the 1995 heat wave in Chicago. *Ann Intern Med* 129: 173–181, 1998. doi:10.7326/0003-4819-129-3-199808010-00001.
32. **Carvalho AS, Rodeia SC, Silvestre J, Povoá P.** Exertional heat stroke and acute liver failure: a late dysfunction. *BMJ Case Rep* 2016: bcr2016214434, 2016. doi:10.1136/bcr-2016-214434.
33. **Wagner M, Kaufmann P, Fickert P, Trauner M, Lackner C, Stauber RE.** Successful conservative management of acute hepatic failure following exertional heatstroke. *Eur J Gastroenterol Hepatol* 15: 1135–1139, 2003. doi:10.1097/00042737-200310000-00013.
34. **Ward MD, King MA, Gabriel C, Kenefick RW, Leon LR.** Biochemical recovery from exertional heat stroke follows a 16-day time course. *PLoS One* 15: e0229616, 2020. doi:10.1371/journal.pone.0229616.
35. **Figiel W, Morawski M, Graöt M, Kornasiewicz O, Niewiński G, Raszęja-Wyszomirska J, Krasnodełbski M, Kowalczyk A, Hołówo W, Patkowski W, Zieniewicz K.** Fulminant liver failure following a marathon: Five case reports and review of literature. *World J Clin Cases* 7: 1467–1474, 2019. doi:10.12998/wjcc.v7.i12.1467.
36. **Morán GAG, Parra-Medina R, Cardona AG, Quintero-Ronderos P, Rodriguez ÉG.** Cytokines, chemokines, and growth factors. In: *Autoimmunity: From Bench to Bedside*, edited by Anaya JM, Shoenfeld Y, Rojas-Villarraga A, Levy RA, Cervera R. Bogota, Colombia: El Rosario University Press, 2013, p. 133–168.
37. **Chaitanya GV, Eeka P, Munker R, Alexander JS, Babu PP.** Role of cytotoxic protease granzyme-b in neuronal degeneration during human stroke. *Brain Pathol* 21: 16–30, 2011. doi:10.1111/j.1750-6339.2010.00426.x.
38. **Hassanshahi G, Patel SS, Jafarzadeh AA, Dickson AJ.** Expression of CXC chemokine IP-10/Mob-1 by primary hepatocytes following heat shock. *Saudi Med J* 28: 514–518, 2007.
39. **Farber JM.** Mig and IP-10: CXC chemokines that target lymphocytes. *J Leukoc Biol* 61: 246–257, 1997.
40. **Dineen SM, Ward JA, Leon LR.** Prior viral illness increases heat stroke severity in mice. *Exp Physiol* 106: 244–257, 2021. doi:10.1113/EP088480.
41. **Liu M, Guo S, Hibbert JM, Jain V, Singh N, Wilson NO, Stiles JK.** CXCL10/IP-10 in infectious diseases pathogenesis and potential therapeutic implications. *Cytokine Growth Factor Rev* 22: 121–130, 2011. doi:10.1016/j.cytogfr.2011.06.001.
42. **Mukhopadhyay I, Saxena DK, Chowdhuri DK.** Hazardous effects of heat from the chrome plating industry: 70 kDa heat shock protein expression as a marker of cellular damage in transgenic *Drosophila melanogaster* (hsp70-lacZ). *Environ Health Perspect* 111: 1926–1932, 2003. doi:10.1289/ehp.6339.

43. Santos-Junior VA, Lollo PCB, Cantero MA, Moura CS, Amaya-Farfan J, Morato PN. Heat shock proteins: protection and potential biomarkers for ischemic injury of cardiomyocytes after surgery. *Braz J Cardiovasc Surg* 33: 291–302, 2018. doi:10.21470/1678-9741-2017-0169.
44. Lu X, Nemoto S, Lin A. Identification of c-Jun NH2-terminal protein kinase (JNK)-activating kinase 2 as an activator of JNK but not p38. *J Biol Chem* 272: 24751–24754, 1997. doi:10.1074/jbc.272.40.24751.
45. Hu Y, Metzler B, Xu Q. Discordant activation of stress-activated protein kinases or c-Jun NH2-terminal protein kinases in tissues of heat-stressed mice. *J Biol Chem* 272: 9113–9119, 1997. doi:10.1074/jbc.272.14.9113.
46. Hibi M, Lin A, Smeal T, Minden A, Karin M. Identification of an onco-protein- and UV-responsive protein kinase that binds and potentiates the c-Jun activation domain. *Genes Dev* 7: 2135–2148, 1993. doi:10.1101/gad.7.11.2135.
47. Morton S, Davis RJ, McLaren A, Cohen P. A reinvestigation of the multisite phosphorylation of the transcription factor c-Jun. *EMBO J* 22: 3876–3886, 2003. doi:10.1093/emboj/cdg388.
48. Dhanasekaran DN, Reddy EP. JNK signaling in apoptosis. *Oncogene* 27: 6245–6251, 2008. doi:10.1038/onc.2008.301.
49. Johnson GL, Nakamura K. The c-jun kinase/stress-activated pathway: regulation, function and role in human disease. *Biochim Biophys Acta* 1773: 1341–1348, 2007. doi:10.1016/j.bbamcr.2006.12.009.
50. Latchoumycandane C, Goh CW, Ong MM, Boelsterli UA. Mitochondrial protection by the JNK inhibitor leflunomide rescues mice from acetaminophen-induced liver injury. *Hepatology* 45: 412–421, 2007. doi:10.1002/hep.21475.
51. Nakagawa H, Maeda S, Hikiba Y, Ohmae T, Shibata W, Yanai A, Sakamoto K, Ogura K, Noguchi T, Karin M, Ichijo H, Omata M. Deletion of apoptosis signal-regulating kinase 1 attenuates acetaminophen-induced liver injury by inhibiting c-Jun N-terminal kinase activation. *Gastroenterology* 135: 1311–1321, 2008. doi:10.1053/j.gastro.2008.07.006.
52. Meriin AB, Yaglom JA, Gabai VL, Zon L, Ganiatsas S, Mosser DD, Zon L, Sherman MY. Protein-damaging stresses activate c-Jun N-terminal kinase via inhibition of its dephosphorylation: a novel pathway controlled by HSP72. *Mol Cell Biol* 19: 2547–2555, 1999 [Erratum in *Mol Cell Biol* 19: 5235, 1999]. doi:10.1128/MCB.19.4.2547.
53. Henderson NC, Pollock KJ, Frew J, Mackinnon AC, Flavell RA, Davis RJ, Sethi T, Simpson KJ. Critical role of c-jun (NH2) terminal kinase in paracetamol-induced acute liver failure. *Gut* 56: 982–990, 2007. doi:10.1136/gut.2006.104372.
54. Gunawan BK, Liu ZX, Han D, Hanawa N, Gaarde WA, Kaplowitz N. c-Jun N-terminal kinase plays a major role in murine acetaminophen hepatotoxicity. *Gastroenterology* 131: 165–178, 2006. doi:10.1053/j.gastro.2006.03.045.
55. Graber CD, Reinhold RB, Breman JG, Harley RA, Hennigar GR. Fatal heat stroke. Circulating endotoxin and gram-negative sepsis as complications. *JAMA* 216: 1195–1196, 1971. doi:10.1001/jama.216.7.1195.
56. Gathiram P, Gaffin SL, Brock-Utne JG, Wells MT. Time course of endotoxemia and cardiovascular changes in heat-stressed primates. *Aviat Space Environ Med* 58: 1071–1074, 1987.
57. Gathiram P, Wells MT, Brock-Utne JG, Gaffin SL. Antilipopolysaccharide improves survival in primates subjected to heat stroke. *Circ Shock* 23: 157–164, 1987.
58. Chow JC, Young DW, Golenbock DT, Christ WJ, Gusovsky F. Toll-like receptor-4 mediates lipopolysaccharide-induced signal transduction. *J Biol Chem* 274: 10689–10692, 1999. doi:10.1074/jbc.274.16.10689.
59. Pradère JP, Hernandez C, Koppe C, Friedman RA, Luedde T, Schwabe RF. Negative regulation of NF- κ B p65 activity by serine 536 phosphorylation. *Sci Signal* 9: ra85, 2016. doi:10.1126/scisignal.aab2820.
60. Beg AA, Sha WC, Bronson RT, Ghosh S, Baltimore D. Embryonic lethality and liver degeneration in mice lacking the RelA component of NF- κ B. *Nature* 376: 167–170, 1995. doi:10.1038/376167a0.
61. Laitano O, Garcia CK, Mattingly AJ, Robinson GP, Murray KO, King MA, Ingram B, Ramamoorthy S, Leon LR, Clanton TL. Delayed metabolic dysfunction in myocardium following exertional heat stroke in mice. *J Physiol* 598: 967–985, 2020. doi:10.1113/JP279310.
62. Wada T, Stepniak E, Hui L, Leibbrandt A, Katada T, Nishina H, Wagner EF, Penninger JM. Antagonistic control of cell fates by JNK and p38-MAPK signaling. *Cell Death Differ* 15: 89–93, 2008. doi:10.1038/sj.cdd.4402222.
63. Campbell JS, Argast GM, Yuen SY, Hayes B, Fausto N. Inactivation of p38 MAPK during liver regeneration. *Int J Biochem Cell Biol* 43: 180–188, 2011. doi:10.1016/j.biocel.2010.08.002.
64. Mendelson KG, Contois LR, Tevosian SG, Davis RJ, Paulson KE. Independent regulation of JNK/p38 mitogen-activated protein kinases by metabolic oxidative stress in the liver. *Proc Natl Acad Sci USA* 93: 12908–12913, 1996. doi:10.1073/pnas.93.23.12908.
65. Garcia CK, Mattingly AJ, Robinson GP, Laitano O, King MA, Dineen SM, Leon LR, Clanton TL. Sex-dependent responses to exertional heat stroke in mice. *J Appl Physiol* (1985) 125: 841–849, 2018. doi:10.1152/jappphysiol.00220.2018.
66. van Bogaert MJ, Groenink L, Oosting RS, Westphal KG, van der Gugten J, Olivier B. Mouse strain differences in autonomic responses to stress. *Genes Brain Behav* 5: 139–149, 2006. doi:10.1111/j.1601-183X.2005.00143.x.
67. Zhao Z, Cao J, Niu C, Bao M, Xu J, Huo D, Liao S, Liu W, Speakman JR. Body temperature is a more important modulator of lifespan than metabolic rate in two small mammals. *Nat Metab* 4: 320–326, 2022. doi:10.1038/s42255-022-00545-5.